Lower-lying states of hydrogenic impurity in lens-shaped and semi-lens-shaped quantum dots

2007 J. Phys.: Condens. Matter 19 136208

(http://iopscience.iop.org/0953-8984/19/13/136208)

IOP PUBLISHING JOURNAL OF PHYSICS: CONDENSED MATTER

J. Phys.: Condens. Matter **19** (2007) 136208 (14pp) doi:10.1088/0953-8984/19/13/136208

Lower-lying states of hydrogenic impurity in lens-shaped and semi-lens-shaped quantum dots

M Barati[1], **M R K Vahdani and G Rezaei**

Department of Physics, College of Sciences, Shiraz University, Shiraz 71454, Iran

E-mail: barati@susc.ac.ir

Received 13 December 2006, in final form 3 February 2007
Published 13 March 2007
Online at stacks.iop.org/JPhysCM/19/136208

Abstract

The lower-lying states of a hydrogenic impurity, located at the centre of an infinite barrier lens-shaped quantum dot (LSQD), are calculated analytically in parabolic rotational coordinates. The solutions are obtained directly using the Frobenius method and by transforming the separated differential equations into the Whittaker equation. Results are given for both symmetric and asymmetric LSQDs. It is found that the energy states of the system are positive for a very small LSQD and decrease as the size of the dot increases. They become negative as the size increases, and approach the energy states of a free hydrogen atom. Also symmetric and antisymmetric eigenfunctions have been constructed for a hydrogenic impurity in a symmetric LSQD. Antisymmetric eigenfunctions can be used as eigenfunctions of a hydrogenic impurity located at the surface of a semi-LSQD.

(Some figures in this article are in colour only in the electronic version)

1. Introduction

Many recent research developments have been devoted to nanostructured semiconductor materials. Quantum wires (QWs) or quantum dots (QDs) show improved properties as compared to semiconductor quantum wells for high-performance optoelectronic devices [1–3]. The effects of quantum size in the physical properties of these structures have been investigated both experimentally [4] and theoretically [5]. A driving force has been the attainment of atomic-like discrete energy levels for the electrons, as opposed to the Bloch energy bands in crystals. Two directions in research can be identified. One involves the numerical solution of the multi-band theory of the electron in realistic shapes such as pyramidal QDs [6]. The other involves obtaining analytic or semi-analytic results for various QD shapes of somewhat higher symmetry. The latter is often done using an infinite barrier and within a one-band effective-mass

[1] Author to whom any correspondence should be addressed.

approach. The goal of the latter approach is to obtain a better physical picture of the role of the shape on the electronic properties [7]. As a recent example of the use of the latter methodology, Cantele *et al* [8] discovered topological surface states in spheroidal QDs. Some of the other shapes considered so far are spheres [9], cones [10], rectangles [11], discs or cylinders [12], and domes or flat lenses [13].

Deposition of $In_xGa_{1-x}As$ on GaAs ($x = 0.6$ [14, 15]) and InAs on GaAs [16] and InAs on InP [17] produces semi-lens-shaped quantum dots. For example, deposition of InAs on GaAs in the Stranski–Krastanow growth mode produces lens-shaped quantum dots 20 nm in diameter, 6 nm high, with a density in the 10^9 cm^{-2} range [16]. These quantum dots are used for laser applications and to improve the characteristics of laser diodes [17]. They can be well described by the geometry imposed by parabolic rotational coordinates.

Since Bastards pioneering work on the donor impurity in a semiconductor quantum well, the properties of impurities have always been of great interest to researchers [18]. Many authors have extended their research to impurities in low-dimensional structures [19, 20]. Chuu *et al* [21] studied the hydrogen-like impurities in a QD and QW, considering infinite-confinement situations, and Szafran *et al* [22] studied the hydrogen-like impurities in a QD considering finite-confinement situations. Since it is impossible to obtain an analytical solution for the Schrödinger equation for an impurity in a low-dimensional system, approximation methods have to be used; among these, the variational approach is the one extensively used. In recent publications [23, 24], one of authors of this paper developed a trial wavefunction especially tailored for QW structures.

The energy eigenfunctions and eigenvalues of an electron confined in a lens-shaped quantum dot for three particular sizes of symmetric and antisymmetric shapes in the effective mass approximation have recently been investigated by Lew Yan Voon and Willatzen (VW) [7]. In section 2, the work by VW will be extended and generalized for all sizes of LSQD by obtaining two simple expressions for the eigenfunctions in terms of the characteristic parameters. The results will be presented in section 3 with some comments on the parity and on the eigenfunctions of a semi-LSQD.

In order to study the hydrogen impurity states in LSQDs, first the problem of a free hydrogen atom in parabolic rotational (PR) coordinates [25] will be reviewed, generalized, and compared with the method of calculation in spherical coordinates in section 4. It is clear that such coordinates are quite suitable for studying the energy eigenvalues and eigenfunctions of a hydrogen-like impurity located at the centre of an LSQD. The results are presented and discussed in section 5 and the conclusion is given in section 6.

2. Schrödinger equation in parabolic rotational coordinates for a particle confined in an LSQD

In this section the eigenfunctions and eigenvalues of a particle confined in a closed region of space with parabolic rotational geometry are calculated. It is considered that the lens-shaped quantum dot has rotational symmetry around the z-direction. Such a surface can be described in PR coordinates by ξ, η and φ, which are related to the Cartesian coordinates as

$$\begin{aligned} x &= \xi\eta\cos(\varphi), \\ y &= \xi\eta\sin(\varphi), \\ z &= 1/2(\eta^2 - \xi^2), \end{aligned} \tag{1}$$

with $0 \leqslant \xi < \infty$, $0 \leqslant \eta < \infty$, and $0 \leqslant \varphi < 2\pi$. The LSQD is limited by the surfaces S_1 and S_2, which are identified by

$$\begin{aligned} &S_1\colon \xi = \xi_0, \\ &S_2\colon \eta = \eta_0 = \alpha\xi_0, \end{aligned} \tag{2}$$

where α is an arbitrary coefficient.

In order to see how the energy states of a electron confined in an LSQD are affected by the presence of the central attractive hydrogen-type potential, first the energy states of a electron confined in an LSQD are investigated. In this case the Schrödinger equation and the boundary conditions are given as (hereafter we use the effective Rydberg unit, therefore the lengths and energies are expressed in terms of effective Bohr radius $a_0 = \epsilon^2/(m^* e^2)$ and effective Rydberg $E_0 = e^2/(2\epsilon a_0)$ respectively)

$$-\nabla^2\psi(\xi,\eta,\varphi) = E\psi(\xi,\eta,\varphi), \tag{3}$$

$$\psi(\xi,\eta,\varphi)|_{\xi=\xi_0,\eta=\eta_0} = 0. \tag{4}$$

In the general case (finite potential barrier), the Hamiltonian is only separable in (ξ,η) and φ coordinates, and $\psi(\xi,\eta,\varphi) = \chi(\xi,\eta)\times \mathrm{e}^{\mathrm{i}m\varphi}$ are general solutions of the problem. In the case of an infinite potential barrier, however, the Hamiltonian is separable in ξ, η, and φ coordinates, and the wavefunction appears as a product of functions of independent variables,

$$\psi(\xi,\eta,\varphi) = Nf(\xi)g(\eta)\,\mathrm{e}^{\mathrm{i}m\varphi}, \tag{5}$$

where m is an integer and N is the normalization constant. The functions f and g are solutions of two coupled differential equations with a separation constant A [26]:

$$\frac{1}{\xi}\frac{\mathrm{d}}{\mathrm{d}\xi}\left(\xi\frac{\mathrm{d}f}{\mathrm{d}\xi}\right) + \left(-\frac{m^2}{\xi^2} + k^2\xi^2 + A\right)f = 0, \tag{6}$$

$$\frac{1}{\eta}\frac{\mathrm{d}}{\mathrm{d}\eta}\left(\eta\frac{\mathrm{d}g}{\mathrm{d}\eta}\right) + \left(-\frac{m^2}{\eta^2} + k^2\eta^2 - A\right)g = 0, \tag{7}$$

where $k^2 = E$. The solution can be written as [7, 27, 28]

$$\begin{aligned} f(\xi) &= \frac{W\left(\frac{\mathrm{i}A}{4k}, \frac{m}{2}, \mathrm{i}k\xi^2\right)}{\xi}, \\ g(\eta) &= \frac{W\left(\frac{-\mathrm{i}A}{4k}, \frac{m}{2}, \mathrm{i}k\eta^2\right)}{\eta}, \end{aligned} \tag{8}$$

where $W(a,c,x)$ is the regular Whittaker function. The value of k^2 and A can be obtained by imposing the boundary conditions (4) [7, 29]:

$$W\left(\frac{\mathrm{i}A}{4k}, \frac{m}{2}, \mathrm{i}k\xi_0^2\right) = W\left(\frac{-\mathrm{i}A}{4k}, \frac{m}{2}, \mathrm{i}k\eta_0^2\right) = 0. \tag{9}$$

This can be simplified as

$$W\left(\mathrm{i}a, \frac{m}{2}, \mathrm{i}c\right) = W\left(-\mathrm{i}a, \frac{m}{2}, \mathrm{i}\alpha^2 c\right) = 0, \tag{10}$$

where $a = \frac{A}{4k}$ and $c = k\xi_0^2$. Therefore

$$\begin{aligned} E &= \frac{c^2}{\xi_0^4}, \\ A &= \frac{4ac}{\xi_0^2}. \end{aligned} \tag{11}$$

For any specific value of $m(0, \pm1, \pm2, \ldots)$ a linear combination of equations (10) will lead to a function f which depends on a, c and the parameter α, i.e. $f(a,c;\alpha) = 0$. As one expects, only for some specific values of a does there exist a solution for f, for some value of c, corresponding to the energy eigenvalues of the dot.

Table 1. Lowest (a, c) values for a symmetric LSQD ($\alpha = 1.0$) and $|m| = 0$.

a	c	a	c	a	c	a	c
0	±4.810	0.428	±7.873	0.917	±10.892	1.460	±13.870
0	±11.040	0.363	±14.154	0.782	±17.238	1.255	±20.291
0	±17.307	0.313	±26.715	0.713	±23.540	1.146	±26.624
0	±23.583	0.299	±32.996	0.670	±29.832	1.024	±39.229

Table 2. Lowest (a, c) values for a symmetric LSQD ($\alpha = 1.0$) and $|m| = 1$.

a	c	a	c	a	c	a	c
0	±14.031	0.689	±10.773	1.308	±13.784	1.917	±16.750
0	±20.347	0.568	±17.155	1.120	±20.225	1.652	±23.263
0	±26.647	0.509	±23.476	1.005	±26.571	1.506	±29.642
0	±32.941	0.472	±29.780	0.937	±32.888	1.409	±35.976

Table 3. Lowest (a, c) values for a symmetric LSQD ($\alpha = 1.0$) and $|m| = 2$.

a	c	a	c	a	c	a	c
0	±12.566	0.581	±9.357	1.138	±12.362	1.710	±15.327
0	±18.850	0.484	±15.679	0.968	±18.751	1.474	±21.793
0	±25.133	0.436	±21.974	0.880	±25.071	1.345	±28.146
0	±31.416	0.407	±28.263	0.823	±31.373	1.260	±34.466

Table 4. Lowest (a, c) values for an asymmetric LSQD ($\alpha = 1.96$) and $|m| = 0$.

a	c	a	c	a	c	a	c
0.238	3.340	5.321	−0.071	7.644	0.468	9.650	0.167
0.940	5.624	7.295	−0.343	9.964	1.133	11.973	0.703
1.764	7.887	9.248	−0.641	12.271	1.889		
2.638	10.125	11.18	−0.967				

Table 5. Lowest (a, c) values for an asymmetric LSQD ($\alpha = 1.96$) and $|m| = 1$.

a	c	a	c	a	c	a	c
4.400	0.447	6.361	−0.016	8.756	0.714	10.744	0.309
6.717	1.291	8.300	−0.387	11.090	1.464	13.105	0.971
8.981	2.163	10.226	−0.740	13.396	2.259	15.443	1.681
11.215	3.060	12.139	−1.096	15.679	3.088	17.764	2.436

3. Results and discussion

3.1. LSQD

Two types of structure are studied: symmetric and asymmetric LSQDs. The symmetric LSQD is obtained for $\alpha = 1$, with the plane of intersection of the two paraboloids at $z = 0$. For $\alpha \neq 1$, the two surfaces have different curvatures, and therefore the intersection plane shifts vertically away from $z = 0$. The calculated results for the lowest energies for symmetric ($\alpha = 1.0$) and asymmetric ($\alpha = 1.96$) LSQDs and for $|m| = 0, 1, 2$ are given in tables 1–3 and 4–6 respectively.

Table 6. Lowest (a, c) values for an asymmetric LSQD ($\alpha = 1.96$) and $|m| = 2$.

a	c	a	c	a	c	a	c
5.389	0.645	7.361	0.075	9.287	−0.372	11.799	0.453
7.749	1.596	9.813	0.935	11.199	−0.778	14.192	1.207
10.026	2.519	12.167	1.758	13.100	−1.169		
12.266	3.447	14.480	2.596				

Table 7. Lowest (a, c) values for a symmetric GaAs LSQD ($\xi_0^2 = \eta_0^2 = 70$ Å).

	Our results		Reference [7]	
	a (Å^{-1})	c (Å^{-1})	a (Å^{-1})	c (Å^{-1})
$m = 0$	0	0.0687	0	0.0687
	0	0.1577	0	0.1577
	0	0.2472	0	0.2473
$m = 0$	0.193	0.1125	0.191	0.1122
$m = 1$	0	0.0898	0	0.0898

The presented method, as discussed before, is applicable for all values of ξ_0. The results are completely consistent with those given by VW [7] for some specific values of ξ_0 geometries (see table 7). In this calculation, the effective mass for GaAs, $m^* = 0.067m_0$, where m_0 is the rest mass of a free electron, is used.

Figures 2 and 3 show the size dependence of A and E of the ground, the first, the second and the third energy states. As is seen from equation (11), E and A decrease as $\frac{1}{\xi_0^4}$ and $\frac{1}{\xi_0^2}$, respectively, as ξ_0 increases.

3.2. States in a semi-LSQD

LSQDs have some basic spatial symmetries. They all have rotational and mirror symmetry about the z-axis; only a symmetric LSQD has, in addition, a reflection symmetry with respect to the $z = 0$ plane. The symmetry about the z-axis allows two-fold degeneracies. However, a closer look at equations (5) and (8) shows that, for $\alpha = 1$, the eigenfunctions, in contrast to the eigenfunctions of a spherical QD, are asymmetric with respect to the $z = 0$ plane. The reflection symmetry guarantees that the states of the symmetric LSQD can be classified as even or odd functions of z.

In PR coordinates, the $z \to -z$ transformation, as seen from equation (1), is equivalent to $\xi \to \eta$ or $A \to -A$ in equation (8). Therefore, the eigenfunctions with odd and even parity with respect to $z = 0$ plane are given as

$$\begin{aligned}\Psi^{\pm}_{A,m,k}(\xi,\eta,\phi) &= \frac{N}{\sqrt{2}}(f(\xi)g(\eta) \pm f(\eta)g(\xi))\,\mathrm{e}^{\mathrm{i}m\phi} \\ &= \frac{N}{\sqrt{2}}\left[\frac{W(\frac{\mathrm{i}A}{4k},\frac{m}{2},\mathrm{i}k\xi^2)W(\frac{-\mathrm{i}A}{4k},\frac{m}{2},\mathrm{i}k\eta^2)}{\eta\xi}\right. \\ &\quad \left. \pm \frac{W(\frac{-\mathrm{i}A}{4k},\frac{m}{2},\mathrm{i}k\xi^2)W(\frac{\mathrm{i}A}{4k},\frac{m}{2},\mathrm{i}k\eta^2)}{\eta\xi}\right]\mathrm{e}^{\mathrm{i}m\phi}. \end{aligned} \tag{12}$$

On the other hand, since $\Psi^{-}_{A,m,k}(\xi,\eta,\phi)$ is odd under $z \to -z$ transformation, it is zero at the $z = 0$ plane. Therefore it is also the eigenfunction of the Hamiltonian of a semi-LSQD (see figure 1) with the same eigenvalues.

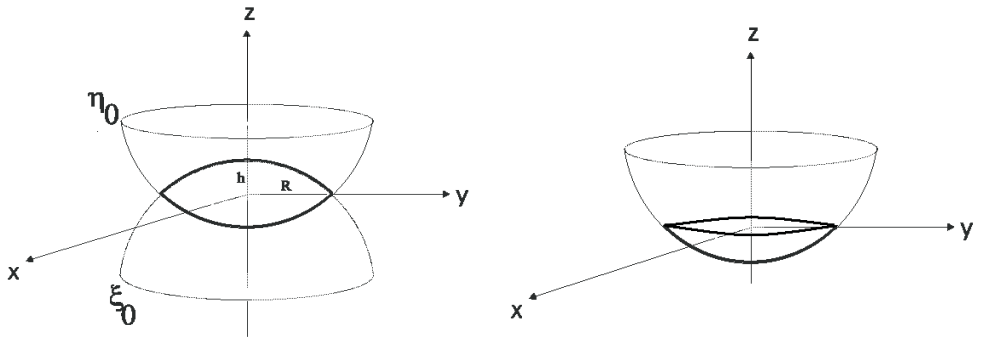

Figure 1. The lens-shaped QD (left) and semi-lens-shaped QD (right) in PR coordinates.

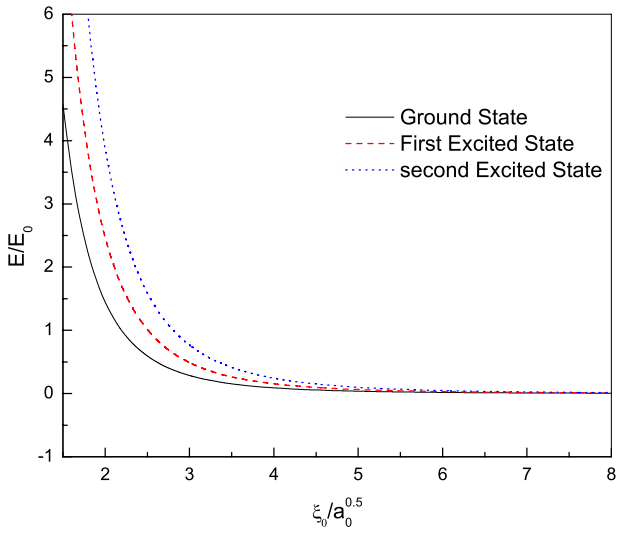

Figure 2. The size dependence of the energy E of the ground, first, second, and third excited states of an electron confined in an LSQD.

4. Hydrogenic impurity confined in an LSQD

4.1. Theory

We assume the effective mass approximation of the Hamiltonian for an impurity located at the centre of an LSQD and infinite-barrier potential, i.e., $V_c = 0$ inside and $V_c = \infty$ outside the LSQD. The Hamiltonian can be written as

$$H = -\nabla^2 - \frac{2}{|\mathbf{r}|}. \tag{13}$$

The PR coordinates allow one to carry out the calculations in quite a general form for LSQDs. Before calculating the electronic states in an LSQD, it is helpful to solve the Schrödinger equation for a free hydrogen atom ($V_c = 0$ everywhere) in PR coordinates.

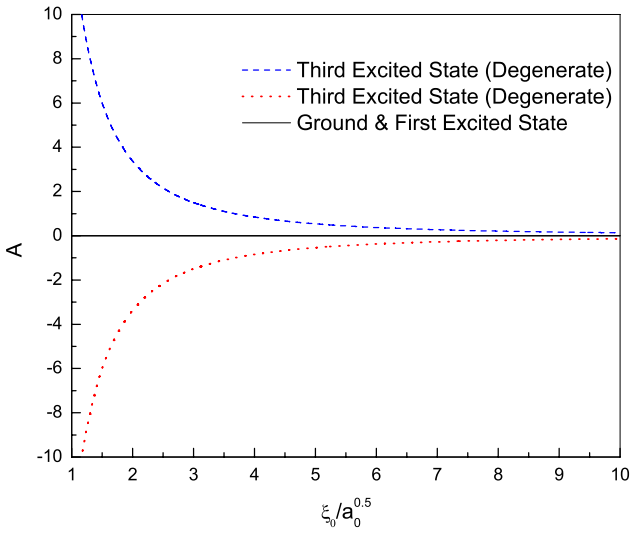

Figure 3. The size dependence of the energy A of the ground, first, second, and third excited states of an electron confined in an LSQD.

4.2. Hydrogen atom in PR coordinates

In PR coordinates, the Schrödinger equation is given as

$$\frac{1}{(\xi^2+\eta^2)^2}\left[\frac{1}{\xi}\frac{\partial}{\partial\xi}\left(\xi\frac{\partial\psi}{\partial\xi}\right)+\frac{1}{\eta}\frac{\partial}{\partial\eta}\left(\eta\frac{\partial\psi}{\partial\eta}\right)\right]+\frac{1}{\xi^2\eta^2}\frac{\partial^2\psi}{\partial\varphi^2}+\frac{2e^2}{(\xi^2+\eta^2)}\psi+E\psi=0. \quad (14)$$

This equation is separable [26], and therefore the wavefunction can be written as

$$\psi(\xi,\eta,\varphi)=f_+(\xi)f_-(\eta)\,\mathrm{e}^{\mathrm{i}m\varphi}. \quad (15)$$

Equation (16) is now separated into two ordinary differential equations:

$$\frac{1}{x_\pm}\frac{\mathrm{d}}{\mathrm{d}x_\pm}\left(x_\pm\frac{\mathrm{d}f_\pm}{\mathrm{d}x_\pm}\right)+\left(-\frac{m^2}{x_\pm^2}+k^2x_\pm^2+A_\pm\right)f_\pm=0, \quad (16)$$

where $x_+=\xi$, $x_-=\eta$, $k^2=E$ and $A_\pm$ are arbitrary constants subject to the condition $A_++A_-=4$. It is useful to introduce a constant c' such that

$$A_\pm=2\pm c'. \quad (17)$$

For calculating the bound states of the system, it is helpful to define a parameter κ such that $\kappa^2=-k^2=|E|$, and hence

$$\frac{1}{x_\pm}\frac{\mathrm{d}}{\mathrm{d}x_\pm}\left(\xi\frac{\mathrm{d}f_\pm}{\mathrm{d}x_\pm}\right)+\left(-\frac{m^2}{x_\pm^2}-\kappa^2x_\pm^2+A_\pm\right)f_\pm=0. \quad (18)$$

The solutions are

$$f_\pm(x_\pm)=\frac{W(\kappa_\pm,\mu,\rho_\pm)}{x_\pm} \quad (19)$$

where

$$\begin{aligned}\kappa_\pm&=\frac{2\pm c'}{4\sqrt{E}},\\ \rho_\pm&=\kappa x_\pm^2=\sqrt{E}x_\pm^2,\\ \mu&=\frac{m}{2}.\end{aligned} \quad (20)$$

Table 8. The allowed values of quantum numbers m and n' for $n = 1, 2$, and 3 values of principal quantum number.

n	Max. of $\|m\|$	m	Max. of $\|n'\|$	n'
1	0	0	0	0
2	1	0	1	±1
		±1	0	0
3	2	0	2	0
				±2
		±1	1	±1
		±2	0	0

The nominator of equations (23) and (24) can be written as [26]

$$\mathrm{nom}(f_\pm) = \mathrm{e}^{-\frac{\rho_\pm}{2}} \rho_\pm^{\mu+\frac{1}{2}} \sum_{n=0}^{\infty} \frac{(\mu - \kappa_\pm + \frac{1}{2})_n}{(2\mu+1)_n} \frac{\rho_\pm^n}{n!}, \tag{21}$$

respectively, where $(a)_n = a(a+1)\cdots(a+n-1)$. These relations show that the solutions are not well behaved at infinity, unless they terminate. This means that for a given m, for some $n = n_i$ we must have

$$\mu - \kappa_\pm + \tfrac{1}{2} = -n_\pm, \tag{22}$$

or

$$\frac{|m|}{2} - \frac{2 \pm c}{4\sqrt{E}} + \frac{1}{2} = -n_\pm. \tag{23}$$

Therefore

$$\begin{aligned} \frac{1}{\sqrt{|E|}} &= n_+ + n_- + |m| + 1, \\ c' &= \frac{2(n_+ - n_-)}{n_+ + n_- + |m| + 1}. \end{aligned} \tag{24}$$

By introducing two *new quantum numbers n and* n' such that

$$\begin{aligned} n &= n_+ + n_- + |m| + 1, \\ n' &= n_+ - n_-, \end{aligned} \tag{25}$$

it follows from the fact that $|m|, n_+, n_- \geqslant 0$ that: (1) $n \geqslant 0$, (2) n and n' are integers and can be written as

$$n_\pm = -\tfrac{1}{2}(|m| - n \mp n' + 1), \tag{26}$$

and (3)

$$\begin{aligned} |E| &= \frac{1}{n^2}, \\ c' &= \frac{2n'}{n}. \end{aligned} \tag{27}$$

Hence, for any value of n, there exist some restrictions on the values of n' and m. The allowed values of m and n' for $n = 1, 2$ and 3 are presented in table 8.

The energy eigenvalues of a hydrogen atom are exactly the same as those obtained by the standard method in spherical polar (SP) coordinates. This supports the method which will be applied in the next section for calculating the hydrogenic impurity state in an LSQD.

As is expected and inferred from table 8, states are degenerate in a way that, for a given n, there exist $-(n-1)\ldots(n-1)$ possible values for m, and for each m there are $n-|m|$ degeneracies. Thus the total number of degeneracies for a given energy is

$$\sum_{m=-(n-1)}^{(n-1)}(n-|m|)=n^2. \tag{28}$$

Therefore, the degree of degeneracy of the nth state, as it must be, is the same as in SP coordinates [25].

The eigenfunctions in PR coordinates, in contrast to the eigenfunctions in SP coordinates, are asymmetric with respect to the $z=0$ plane, except for those with $n'=0$. For $n'>0$, a larger portion of the charge distribution of the electron lies on the positive side of z, and vice versa [25]. Equations (20) and (19) show that the $\xi \leftrightarrow \eta$ transformation is equivalent to $c' \to -c'$ or equivalently $n' \to -n'$ transformations. Therefore, one can introduce a linear combination of eigenfunctions (15), which are simultaneous eigenfunctions of the Hamiltonian and parity operator π_z as follows:

$$\begin{aligned}\Psi^{\pm}_{n,m,|n'|}(\xi,\eta,\phi) &= \frac{N}{\sqrt{2}}(f_+(\xi)f_-(\eta)\pm f_+(\eta)f_-(\xi))\,\mathrm{e}^{\mathrm{i}m\phi}\\ &= \frac{N}{\sqrt{2}}\left[\frac{W(\frac{n+n'}{2},\frac{m}{2},\frac{\xi^2}{n})W(\frac{n-n'}{2},\frac{m}{2},\frac{\eta^2}{n})}{\eta\xi}\right.\\ &\quad\left.\pm\frac{W(\frac{n-n'}{2},\frac{m}{2},\frac{\xi^2}{n})W(\frac{n+n'}{2},\frac{m}{2},\frac{\eta^2}{n})}{\eta\xi}\right]\mathrm{e}^{\mathrm{i}m\phi}.\end{aligned} \tag{29}$$

These eigenfunctions are now symmetric or antisymmetric with respect to the xy-plane. The importance of the particular definition of n' now becomes clear. Since only eigenfunctions with the same values of n and the same values of m but with different signs of n' are combined to produce symmetric and antisymmetric eigenfunctions, n' can still be used as one of the quantum numbers of the system. There is also a close relation between these new eigenfunctions and the eigenfunctions of the hydrogen atom in SP coordinates. Using equation (21), one can easily show that the new eigenfunctions are exactly proportional to the eigenfunctions in SP coordinates. For example,

$$\begin{aligned}\Psi^{+}_{2,0,1}(\xi,\eta,\phi) &\propto R_{20}(r)Y^0_0(\theta,\phi),\\ \Psi^{-}_{2,0,1}(\xi,\eta,\phi) &\propto R_{21}(r)Y^0_1(\theta,\phi).\end{aligned} \tag{30}$$

where $R_{nl}(r)$ and $Y^m_l(\theta,\phi)$ are the radial and the angular parts of the eigenfunction of a state with n, l and m quantum numbers of a free hydrogen atom in SP coordinates.

4.3. Hydrogenic impurity in an LSQD

Now we return to our original problem of a hydrogenic impurity in an LSQD. Consider an impurity which is located at the centre of an LSQD. The energy eigenvalues and eigenfunctions (i.e. E and c'), can be determined by the method applied in section 2 and by imposing the boundary conditions:

$$W(\kappa_1,\mu,\kappa\xi_0^2)=W(\kappa_2,\mu,\kappa\alpha^2\xi_0^2)=0. \tag{31}$$

It is more convenient to introduce two parameters a and b, where $E=1/(n+a)^2$ and $c'=2(n'+b)/(n+a)$, in which n and n' are the quantum numbers defined in the problem of the free hydrogen atom in subsection 4.2. One expects that a and b approach zero as ξ_0 approaches infinity. Equation (31) can be solved simultaneously to find a and b and therefore E and c' as a function of ξ_0.

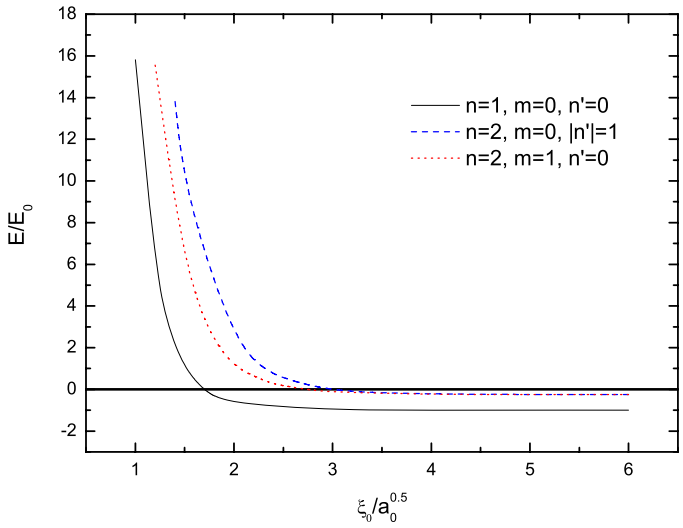

Figure 4. The energy of the ground, first, and second excited states of a hydrogenic impurity in a symmetric LSQD as a function of ξ_0.

5. Results and discussion

5.1. LSQDs

The lower-lying states and binding energies of a hydrogenic impurity located at the centre $(x, y, z = 0)$ of an LSQD are calculated for different values of ξ_0. For clarity we have limited all our graphs to $\xi_0 < 6a_0^{0.5}$. Again two types of structure are studied: symmetric ($\alpha = 1$) and asymmetric ($\alpha \neq 1$) LSQDs. The variation of the binding energy with respect to ξ_0 is plotted in figure 6. It is obvious that as $\xi_0 \to \infty$ all the eigenvalues tend, as they should, to the corresponding eigenvalues of the free hydrogenic impurity. Therefore, hereafter we are using the quantum numbers of the free hydrogenic impurity to refer to the corresponding states of the hydrogenic impurity in the LSQD.

5.1.1. Symmetric LSQDs. Figure 4 shows the splitting, arrangement, and the variation of the energy eigenvalues of the states $n = 1$, and $n = 2$. Since

(1) the potential barrier is invariant with respect to rotation about the z-axis, and
(2) it has mirror symmetry with respect to the xy-plane,

it is expected that eigenstates with the same values of n and the same values of n' but with different signs of m, which are degenerate for a free hydrogen impurity, be degenerate for a hydrogen impurity in an LSQD. Also, the eigenstates with similar values of n and similar values of m but with different signs of n' must be degenerate for the hydrogen impurity in an LSQD. Figure 4 shows these features for states with $n = 2$. It is obvious that eigenstates with $n = 2, m = \pm 1, n' = 0$ and $n = 2, m = 0, n' = \pm 1$, which are degenerate for a free hydrogen impurity, split into two branches in an LSQD with two-fold degeneracy in each branch. It is also interesting to mention that figure 5 actually shows that, as the size of the dot decreases, the effect of the confining potential becomes more dominant than the effect of the Coulombic potential, and therefore the energies become positive and the level spacing increases. This

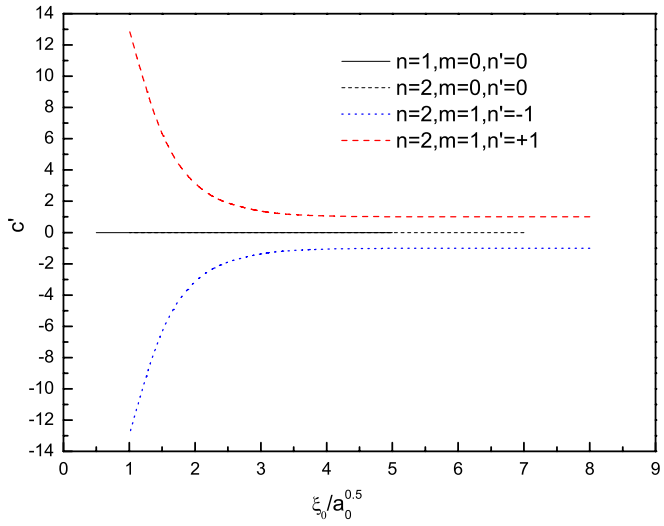

Figure 5. The parameter c' of the ground, first, and second excited states of a hydrogenic impurity in a symmetric LSQD as a function of ξ_0.

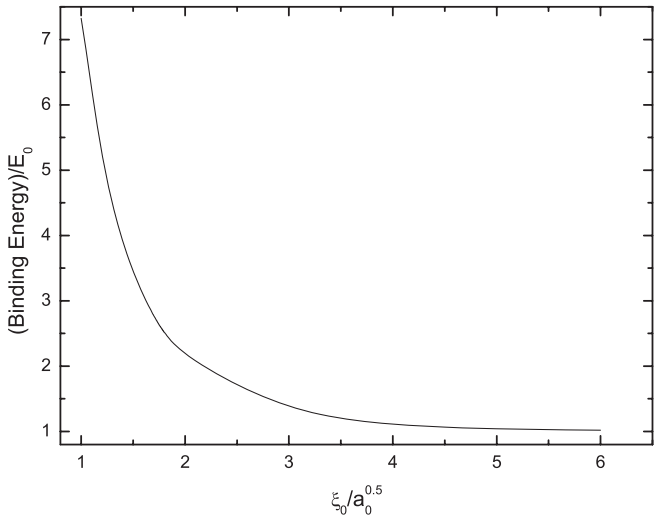

Figure 6. The binding energy of a hydrogenic impurity as a function of the size of a symmetric LSQD.

property, which is seen to be shape independent, has been reported in studies of quantum dots of different shape [30–34].

For $n' = 0$, c' is zero and therefore it is independent of the size of the LSQD (ξ_0) (see figure 5).

We have investigated the shape dependence of the energy spectrum of an LSQD at constant volume in detail. In order to have some idea about the effect of the geometry on the energy states of a dot, the volume dependence of the ground-state energy of the hydrogen impurity in an LSQD is investigated and compared with relevant results for an SQD. The results are presented in figure 9. As is seen from the figure, the ground-state energy in an SQD is smaller than that in an LSQD in the whole range of volume, and the energy difference becomes more

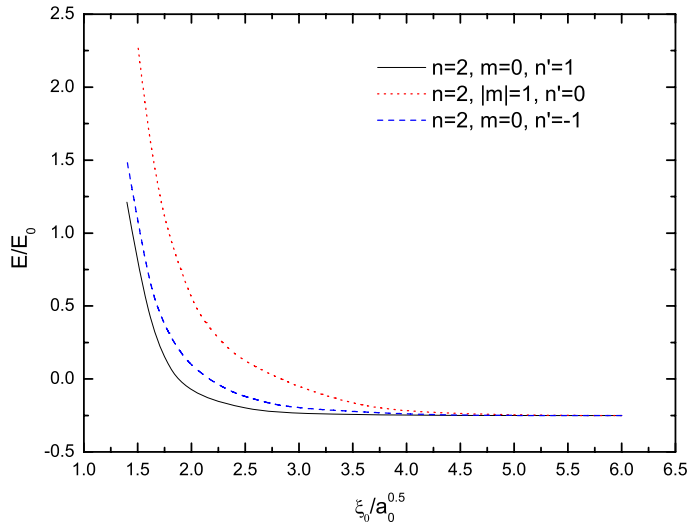

Figure 7. The energy of the ground, first, and second excited states of a hydrogenic impurity in an asymmetric LSQD as a function of ξ_0.

significant for small volumes. The results confirm the fact that the energy states of the system decrease as the level of symmetry of the structure increases. Our results for a semi-LSQD also support this fact that the first excited state energy of the LSQD coincides with the ground state energy of the semi-LSQD.

5.1.2. Asymmetric LSQDs. In this case the dot has only rotational symmetry. Therefore it is expected that only states with the same values of n and the same values of n' but with different sign of m be degenerate in the LSQD. This point has been shown in figures 7, 8 for the states with $n = 2$. This shows that eigenstates with ($n = 2$, $m = \pm 1$, $n' = 0$) and ($n = 2$, $m = 0$, $n' = \pm 1$), which are degenerate for a free hydrogen impurity, now split into three branches in the LSQD, where only one of them is two-fold degenerate.

On the other hand, for $n' = 0$, c' is no longer independent of the size (ξ_0) of the LSQD (see figure 8).

Parity and semi-LSQDs. It is obvious that, like the cases of a confined electron in an LSQD and a free hydrogen impurity, when α is unity and $n' \neq 1$, some of the eigenfunctions (15) of the Hamiltonian (13) are asymmetric with respect to the xy-plane. Similarly to a free electron confined in an LSQD, we introduce symmetric and antisymmetric eigenfunctions (with respect to xy-plane) as follows:

$$\begin{aligned}\Psi^{\pm}_{n,m,n'}(\xi,\eta,\phi) &= \frac{N}{\sqrt{2}}(f(\xi)g(\eta) \pm f(\eta)g(\xi))\,\mathrm{e}^{\mathrm{i}m\phi} \\ &= \frac{N}{\sqrt{2}}\left[\frac{W(\kappa_1,\frac{m}{2},\rho_1)W(\kappa_2,\frac{m}{2},\rho_2)}{\eta\xi}\right. \\ &\quad \left.\pm \frac{W(\kappa_2,\frac{m}{2},\rho_1)W(\kappa_1,\frac{m}{2},\rho_2)}{\eta\xi}\right]\mathrm{e}^{\mathrm{i}m\phi}. \end{aligned} \tag{32}$$

The $\Psi^{-}_{n,m,|n'|}$ has odd parity, and it must vanish at the xy-plane. Since these functions are solutions of the impurity Hamiltonian (13) and approach zero at the surface $z = 0$ for $\xi = \eta = \xi_0$, they are also the solutions of the Schrödinger equation for an impurity located at

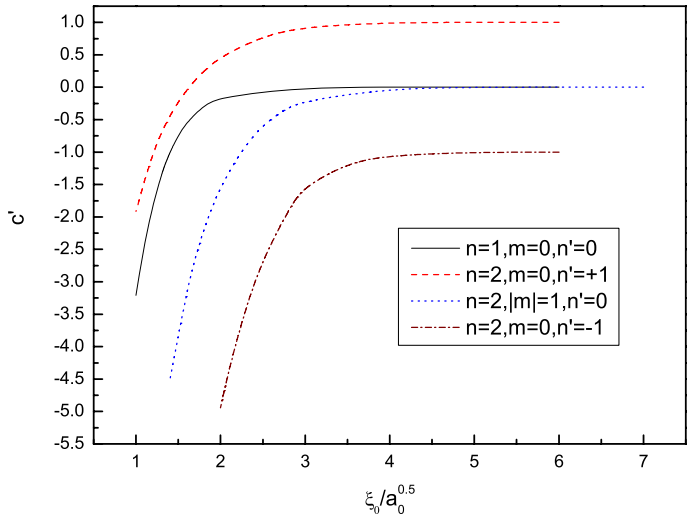

Figure 8. The parameter c' of the ground, first, and second excited states of a hydrogenic impurity in an asymmetric LSQD as a function of ξ_0.

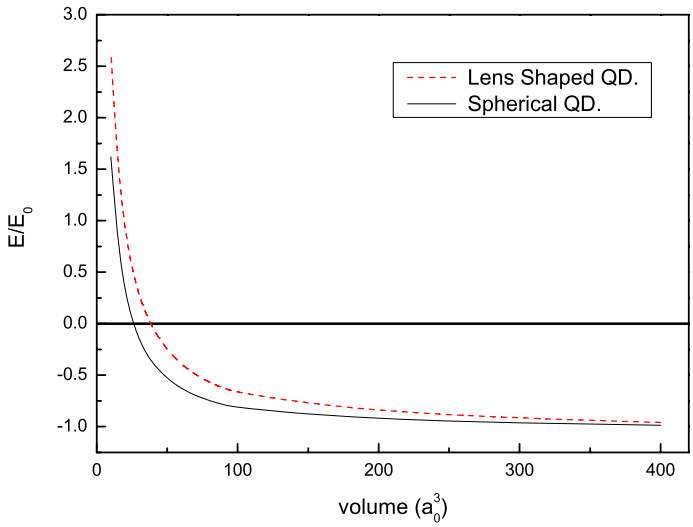

Figure 9. The ground-state energy as a function of volume for SQDs and LSQDs of similar volume.

the centre of the xy-plane in a semi-LSQD (figure 1). Therefore $\Psi^{-}_{n,m,|n'|}$ is the ground state of the semi-LSQD.

6. Conclusions

The energy eigenvalues and eigenfunctions of an electron confined in symmetric, asymmetric and semi-LSQD structures are calculated in general form. It is shown that the energy eigenvalues are inversely proportional to $V^{\frac{2}{3}}$ and as the size of the dot increases, the energy eigenvalues approach zero. Since the calculated energy eigenfunctions of the symmetric LSQD do not show a definite parity π_z, a linear combination of these eigenfunctions which are also

eigenstates of the parity π_z are constructed. The constructed odd eigenfunctions are also the eigenstates of the confined electron in a semi-LSQD, the geometrical structure which is applicable in the study of some active media in quantum dot lasers.

The energy eigenvalues and eigenfunctions of a hydrogenic impurity confined in symmetric, asymmetric and semi-LSQDs are also calculated. The results show that the states and the energy eigenvalues are size dependent and some degree of degeneracies are removed. As the size of the dot increases, the energy eigenvalues and states tend to the energies of a hydrogen atom in the bulk material. As the dot size decreases, the effect of the confining potential becomes more dominant than that of the Coulombic potential and therefore at some small radii the energy eigenvalues become positive and the level spacing increases. This level spacing become considerable at very small radii.

Acknowledgments

We would like to thank Dr M M Golshan and Dr A Poostforoosh for useful discussions and comments. This work has been supported by Shiraz University.

References

[1] Grundmann M, Bimberg D and Ledentsov N N 1998 *Quantum Dot Heterostructures* (Chichester: Wiley)
[2] Sugawara M 1999 *Self-Assembled InGaAs/GaAs Quantum Dots Semiconductors and Semimetals* vol 60 (Toronto: Academic)
[3] Alferov Zh I 1998 Quantum wires and dots show the way forward *III-Vs Rev.* **11** 47
[4] Ramvall P, Tanaka S, Nomura S, Riblet P and Aoyagi Y 1998 *Appl. Phys. Lett.* **73** 1104
[5] Corella Madueno A, Rosas R A, Marin J L and Riera R 1999 *Phys. Low-Dimens. Semicond. Struct.* **5/6** 75
[6] Grundmann M, Stier O and Bimberg D 1995 *Phys. Rev.* B **52** 11969
[7] Lew Yan Voon L C and Willatzen M 2002 *J. Phys.: Condens. Matter* **14** 13667
[8] Cantele G, Ninno D and Iadonisi G 2000 *J. Phys.: Condens. Matter* **12** 9019
[9] Efros Al L and Efros A L 1982 *Sov. Phys.—Semicond.* **16** 772
[10] Marzin J Y and Bastard G 1994 *Solid State Commun.* **92** 437
[11] Lew Yan Voon L C and Willatzen M 1995 *Semicond. Sci. Technol.* **10** 416
[12] Le Goff S and Stebe B 1993 *Phys. Rev.* B **47** 1383
[13] Wojs A, Hawrylak P, Fafard S and Jacak L 1996 *Phys. Rev.* B **54** 5604
[14] Leona R, Lobob C, Liaoc X Z, Zouc J, Cockayne D J H and Fafard S 1999 *Thin Solid Films* **357** 40
[15] Liao X Z, Zou J, Duan X F and Cockayne D J H 1998 *Phys. Rev.* B **58** R4235
[16] Warburton R J, Schulhauser C, Haft D, Schaflein C, Karrai K, Garcia J M, Schoenfeld W and Petroff P M 2002 *Phys. Rev.* B **65** 113303
[17] Frechengues S, Bertru N, Drouot V, Lambert B, Robinet S, Loualiche S, Lacombe D and Ponchet A 1999 *Appl. Phys. Lett.* **74** 3356
[18] Bastard G 1981 *Phys. Rev.* B **24** 4714
[19] Green R L and Bajaj K K 1982 *Solid State Commun.* **45** 825
[20] Maihiot C and Chang Y C 1982 *Phys. Rev.* B **26** 4449
[21] Chuu D S, Hsiao C M and Mei W N 1992 *Phys. Rev.* B **46** 3898
[22] Szafran B, Adamowski J and Stebe B 1998 *J. Phys.: Condens. Matter* **10** 7575
[23] Barati M, Chow J C L, Ummat P K and Datars W R 2001 *J. Phys.: Condens. Matter* **13** 2955
[24] Barati M and Sadeghi E 2001 *Nanotechnology* **12** 277
[25] Bethe H A and Salpeter E E 1957 *Quantum Mechanics of One- and Two-Electron Atoms* (New York: Plenum)
[26] Arfken G 1966 *Mathematical Method for Physicists* (New York: Academic)
[27] Abramowitz M and Stegun I A 1972 *Handbook of Mathematical Functions* (New York: Dover)
[28] Lebedev N N 1972 *Special Functions and Their Applications* (New York: Dover)
[29] Even J and Loualiche S 2004 *J. Phys. A: Math. Gen.* **37** L289–94
[30] Andreev A V, Aleiner I L and Millis A J 2003 *Phys. Rev. Lett.* **91** 056803
[31] Cheng-Ying H 1999 *Chin. J. Phys.* **38** 478
Leo H, Mary J L and Riera R 2005 *Physica* E **27** 385
[32] Kazaryan E M, Petrosyan L S and Sarkisyan H A 2003 *Physica* E **16** 174
[33] Bellessa J and Combescot M 1999 *Solid State Commun.* **111** 275
Bose C and Sarkar K 1998 *Solid-State Electron.* **42** 1661
[34] Barati M, Rezaei G and Vahdani M R K 2007 *Phys. Status Solidi* b at press